J. Condensed Matter Nucl. Sci. 14 (2014) 68–75

Research Article

The Pd + D Co-Deposition: Process, Product, Performance

Stanislaw Szpak*,†

SPAWAR Center San Diego, CA, USA

Abstract

The preparation of electrodes by a co-deposition is discussed in detail. The electrode reactions are identified, the structural features of the deposit are described and the relevant experimental evidence is assembled.
 ISSN 2227-3123

Keywords: Co-deposition

1. Introduction

Recently, I learned that Letts and Hagelstein [1] modified the Szpak protocol to assure a 100% reproducibility in excess heat production. Upon repeated reading, I concluded that I should respond because not all pertinent and available information was used. In their paper, there is the sentence ... *an issue in the Szpak experiment is reflected in the literature in the relative absence of replications showing excess heat due to insufficient loading and poor adhesion.* But, in a publication [2], we discussed the deuterium uptake in detail and have shown that the deuterium loading exceeds 100%. In this communication I present a very different discussion of the Pd + D co-deposition process.

My involvement in the research of the F–P effect dates back to May 1989 when I proposed a variant of the usually employed massive electrodes, viz working electrodes prepared by the Pd + D co-deposition, a process in which the Pd^{2+} and D^{+} ions are electrodeposited onto a substrate which does not absorb deuterium, e.g. Cu, Au, Pt, etc. One obvious reason was to eliminate the charging time. The other, more interesting, was to study the processes that initiate nuclear activity in the polarized Pd/D–D_2O system.

In 1989, not much was known about the Pd + D co-deposition. The development and evaluation of an experimental procedure is not instantaneous. It requires the determination of conditions that maximize its usefulness. In the SPAWAR laboratory we carried out collateral research involving (i) deuterium absorption during co-deposition [2] as well as the electrochemical charging of solid palladium [3,4], (ii) response to change in cathodic over-potential during co-deposition and on solid palladium [5]. We examined the thermal behavior of cells using cathodes prepared by co-deposition using a model which differs from that presented in [1].

*Current address: 3498 Conrad Ave, San Diego, CA 02117, USA. E-mail: stan.szpak@gmail.com
†Retired.

 ISSN 2227-3123

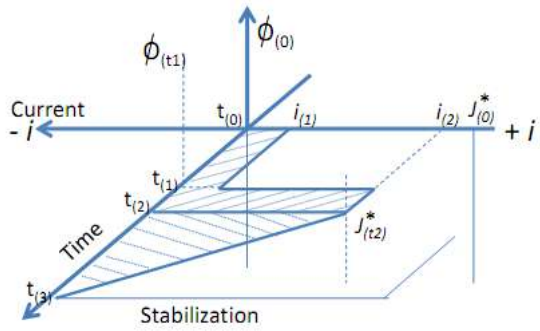

Figure 1. Schematic representation of the co-deposition process.

2. Process

The Pd + D co-deposition may be viewed as a special case of production of alloys by electrochemical processing, i.e. it involves simultaneous deposition of more than one component. To assure good adhesion several steps must be taken, among them (a) selection of the substrate, (b) surface preparation, and (c) co-deposition control. Here, the discussion of co-deposition considers (i) relevant kinetics of electrode reactions and (ii) the art of co-deposition.

2.1. Kinetics of electrode reactions

Briefly, for the production of Pd/D alloy, the relevant reactions are: $Pd^{2+} + 2e^- \rightarrow Pd$ and $D_2O + e^- \rightarrow D + OD^-$. In practice, however, these reactions depend on the electrolyte composition. For co-deposition from a solution containing $PdCl_4^{2-}$ complexes, Naohara [6] found that the reduction of Pd^{2+} proceeds via the reduction of an adsorbed $PdCl_4^{2-}$ complex resulting in a layer-by-layer growth of the Pd film. However, the orderly growth of deposited palladium is disturbed by the adsorbed deuterium generated by the reduction of heavy water. Ohmori et al. [7] using a scanning tunneling microscope, proposed a model where the H^+ ions are adsorbed and reduced at the surface. A part of the adsorbed hydrogen enters the Pd lattice and accumulates around lattice defects. Through this process, the surface is transformed into a modular-like structure.

2.2. The art of Pd + D co-deposition

Figure 1 illustrates the procedure when (i) reduction of $PdCl_4^{2-}$ and D_2O are independent of each other, (ii) electrolyte volume and electrode surface remain constant, (iii) reduction of Pd ions is diffusion controlled and (iv) no other charge transfer reactions occur. Under these conditions the electrode rest potential, $\Phi(0)$, is determined by solution composition. At $t = 0$, a constant cell current, I_1 , is applied.

In practice , the cell current is much smaller than the diffusion limiting current, $I_1 < j_{\text{lim}}$. Note that in Fig. 1, $j*$ denotes the limiting current. This is done to assure an adherent Pd deposit. With the passage of time, the Pd^{2+} ions are depleted, the electrode potential, driven by the cell current, becomes more negative. At $t = t_1$ the cell current is increased to I_2, i.e. to a value very close to the limiting current. This is done to assure a long co-deposition period. When the applied current , I_2, by reducing the concentration of Pd^{2+} ions, becomes the diffusion limiting current (for that concentration) the electrode potential is driven into the region of heavy water instability and at $t = t_2$, the reduction of D^+ ions commences and the co-deposition begins. If the co-deposition is galvanostaticaly controlled and if the cell current exceeds the diffusion limiting current, then, at constant volume and surface area, the Pd^{2+} ions concentration decreases linearly with time. The co-deposition is completed at $t = t_3$.

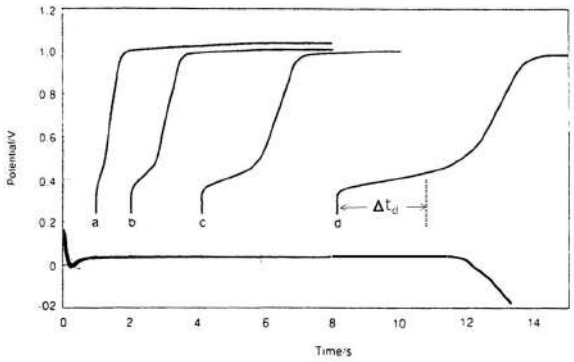

Figure 2. Deuterium up-take during co-deposition. $j_c = -5$ mA cm^{-2} and $j_a = 5$ mA cm^{-2}, with **cell** current reversal at 1, 2, 4 and 8 s.

2.3. Corollary

(1) The Pd + D co-deposition process does not specify (i) the electrolyte concentration except to say that (a) the reduction of Pd^{2+} ions is diffusion controlled[a] , (b) ratio D/Pd reduction determines morphology of the deposit and (c) substrate preparation prior to co-deposition is a crucial component of the process.

(2) Deuterium up-take during co-deposition at constant cell current can be determined from the cathodic and anodic potential/time relationships shown in Fig. 2. The line parallel to the time axis represents potential/time during the co-deposition of the Pd/D film whose composition at a given time depends on how much charge was consumed by Pd^{2+} ions, $Q_{C,1}$ and how much for hydrogen generation, $Q_{C,2}$ which for the atomic ratio D/Pd =1 is 2. Upon switching from cathodic to anodic current, the potential/time curve identifies the following processes: changes in the double layer, desorption and oxidation of deuterium and oxygen evolution.

The atomic ratio D/Pd in is obtained from the ratio $\Delta t_n/\Delta t$ where the subscript n = a, b, c, d, identifies the potential/time curve and Δt is the time needed to obtain the atomic ratio D/Pd =1 at the time of current reversal. The deuterium up-take, expressed as a D/Pd atomic ratio, taken at 1, 2, 4 and 8 seconds of charging are 0.95, 1.07, 1.1 and 1.3.

(3) In the co-deposited Pd/D film the D/Pd = 1.0 atomic ratio is obtained immediately in agreement with and support of thermal data, cf. Fig. 6.

3. Product

The product quality is judged by its performance which, in turn, imposes demands on its construction and/or function. Here, the Pd/D cathodes serve as a seat for heat generation that is nuclear in origin. In practice, one has to answer the following: (i) what is its stability at high cell currents as well as when subjected to highly energetic nuclear reactions, (ii) what is the optimum thickness of the deposit to assure maximum excess heat. The research done in the SPAWAR laboratory indicates that to answer it is necessary to consider (i) the structure of the deposit and its stability, (ii) the interphasse and (iii) the act of absorption.

[a]The composition 0.03 M $PdCl_2$, 0.3 M LiCl in D_2O was found to be satisfactory.

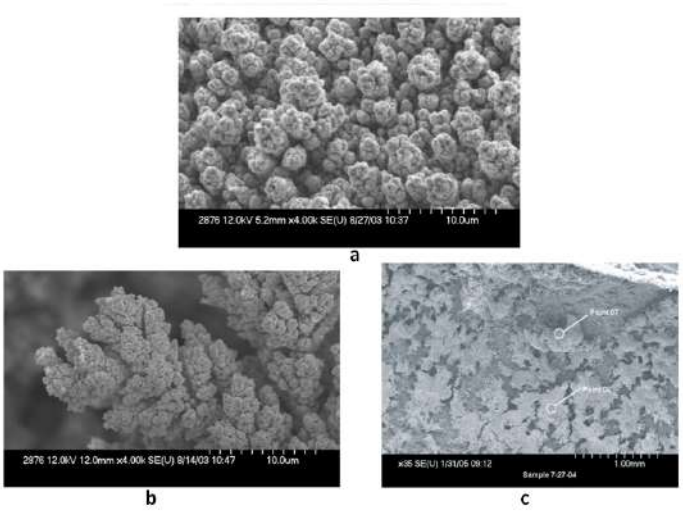

Figure 3. SEM of co-deposited Pd/D film. (a) After completion of co-deposition, (b) exposed to an external electric field, and (c) exposed to magnetic field.

3.1. Structure: Effect of external fields

The structure of the co-deposited Pd/D film from a solution containing $PdCl_4^{2-}$ is shown in Fig. 3. In particular, Fig. 3a is the SEM of the deposit after completion of co-deposition. Its structure did not change when used as a cathode at current densities up to 400 mA cm^{-2}. When the cell was placed in an external electric and magnetic field, its structure has changed as shown in Fig. 3b for an electric field and in Fig.3c in the magnetic field.

(1) Figure 3b is the SEM of the Pd/D cathode shortly after placing the cell in an external electric field which results in swelling and alignment with the field. The initial porous cauliflower-like structure has changed to a columnar arrangement of globules.
(2) The placement of an operating cell in magnetic field changed the globules into pancake-like entities that appear to be firmly affixed to the substrate.

3.2. The interphase

The interphase, $\lambda = \lambda_1 + \lambda_2(\tau)$, is a region separating two homogeneous phases. When the system is in equilibrium, its structure can be defined in terms of physical properties. When the system is not in equilibrium, it is often convenient to discuss its structure in terms of occurring processes, i.e. the interphase can be viewed as an assembly of a set of homogeneous layers whose structure is determined by the operating processes and their relaxation times. To assure their homogeneity, an average value of a particular variable is taken [8]. The imposition of homogeneity of each layer results in its non-autonomous character which arises from the interaction of molecules in adjacent layers. Consequently, changes in any part cause changes throughout the whole region.

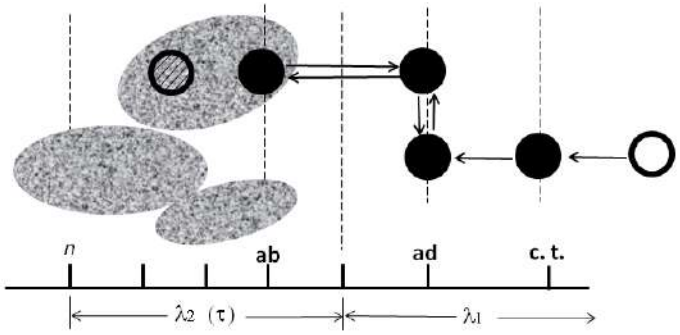

Figure 4. Deuterium crossing the interphase region. (*open circle*) D^+ ion, (*black circle*) deuterium atom, (*shaded circle*) deuteron, ct–charge transfer layer, ab–absorption layer, shaded **areas**- domains.

3.3. Crossing the interphase

Transport of deuterium across the interphase is due to coupling processes at the contact surface followed by transport into the electrode interior, with the concentration of deuterium being larger in the $\lambda_2(\tau)$ segment of the interphase [4]. The solvated D^+ ions are driven toward the negative electrode at the rate determined by the cell current. The electrodeposited deuterium is removed from the contact surface by gas evolution and by absorption. The adsorbed/absorbed deuterium is distributed as follows: (i) The subsurface, D_s is formed just below the topmost layer of Pd atoms and provides the link between the chemisorbed surface atoms, D_a , and the dissolved in metal, D_m, (ii) two energetically different D_a exist, (iii) with chemisorption there is associated surface reconstruction, but only D_s is responsible for its maintenance, (iv) there is an energy barrier separating D_a and D_s which affects transport in both directions. Chemisorbed D_s is responsible for surface reconstruction while absorbed D_s maintain state of reconstruction [9].

3.4. Corollary

(1) Any solid undergoes shape change when the internal forces exceed the elastic limits. In general, three types of forces can be identified as acting during the deformation of a solid. These are (i) internal forces, i.e. forces that obey Newton's law, (ii) applied external forces and (iii) capillary forces (forces that act between the internal and surface molecules, or between solid boundary and the molecules of surrounding liquid). By definition, when the surface forces are not uniformly distributed, they act as external forces. If, in fact, the latter are involved in producing shape changes, Fig. 3, then their action can be magnified by an external electrostatic and/or magnetostatic fields. The relationship between surface forces and the bulk response is given by the Gauss theorem which states that forces acting on any finite body can be reduced to forces applied to the surface and vice versa. It follows that the shape change at constant volume is the result of motion due to forces acting on the surface. Consequently, the deformation is determined by the distribution of surface forces while the rate of deformation, by their magnitude.

(2) The structure of the interphase controls its performance via (a) generation of lattice defects through activities in the λ_1 segment, (e.g. gas bubbling and the associated charge transfer current density), (b) porosity which affects the distribution of the primary charge transfer current density and which determines the useful thickness of the Pd/D deposit.

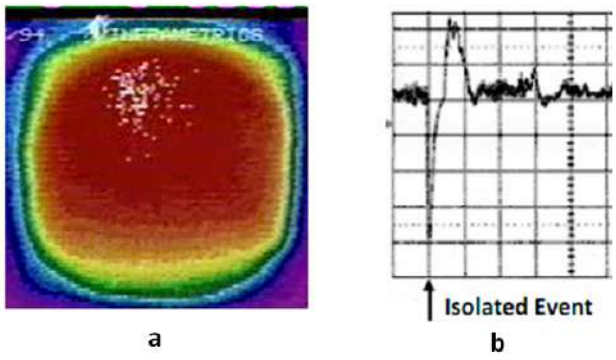

Figure 5. Thermal and mechanical effects. (a) Hot spots and (b) piezoelectric sensor response to a hot spot.

4. Performance

The large quantities of excess enthalpy generation in the Pd/D–D_2O system raised questions: (i) Is the excess enthalpy generation reproducible? (ii) Is the heat source uniform throughout the whole electrode volume or distributed? Experience shows that, if correctly applied, electrodes prepared by the Pd + D co-deposition provide answers: yes to (i) and the discussion based on experimental evidence to (ii).

To confirm the existence of the F–P effect one needs only to establish an excess enthalpy production by calorimetry. But calorimetry, being an integrating procedure, cannot do much more. There are other tools that can add to a better understanding the nature of the polarized Pd/D–D_2O system. One such tool is the infrared (IR) imaging of the surface of an active electrode [10]. The other, prompted by the first, is the use of a pressure sensitive substrate, onto which the Pd/D films are co-deposited, to demonstrate mechanical changes that do occur when an instantaneous and high intensity exothermic reaction takes place [11]. This communication includes a brief discussion of the thermal behavior immediately after beginning of a run.

4.1. Infrared imaging and pressure and temperature wave

Figure. 5a shows the IR image of the cathode and Fig. 5b the associate pressure and temperature waves. The IR imaging shows discrete reaction sites randomly distributed in time and space. The short lived hot spots resemble mini-explosions which, in turn, generate pressure and temperature waves recorded by the piezoelectric sensor. As the solution temperature raises, the hot spots become brighter and an amplified sensor response.

4.2. Initial thermal behavior

The co-deposition starts with endothermic absorption of deuterium. However, within seconds, the endothermic absorption is balanced by an exothermic nuclear reaction, Fig.6, point a. The balance involving endothermic and exothermic process ends at point b.

4.3. Corollary

(1) Existence of domains containing clusters of deuterons or of regions of ordered deuterons dispersed in the Pd lattice that lead to the formation of ordered domains having high D/Pd atomic ratio.

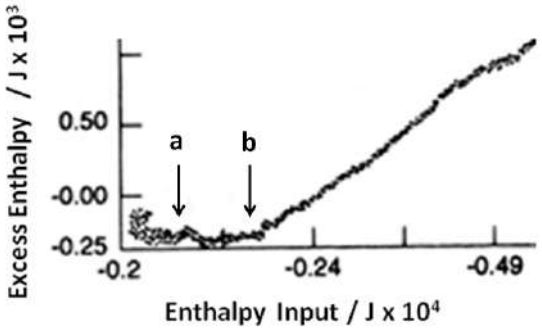

Figure 6. Initial thermal behavior: endothermic absorption – $0 < Q < A$, endothermic absorption balanced by exothermic reaction – $a < Q < b$, exothermic reaction dominates $Q > a$.

(2) The heat source arises from fast chain of nuclear reactions or from a kind of cluster collapse.
(3) The size of the cluster or the rate constant of the chain reaction are temperature dependent

5. Conclusion

The Pd + D co-deposition produces not only effective cathodes but also provides an insight into the conditions that give rise to, and are associated with, the nuclear events that occur within the confines of the Pd lattice. A complete description must include (i) the processes and/or reactions involved, (ii) product and its function and (iii) the performance that determines its effectiveness. In concluding remarks I will address the (i) kinetic aspects very near the starting of co-deposition and (ii) the similarities and differences between the co-deposition described in this communication and that in [1].

5.1. Kinetic aspects at the start of co-deposition

Within seconds after starting co-deposition a series of events takes place. The first set is the accumulation of absorbed deuterium around the lattice defeats, cf. Section 2.1, forming ordered clusters of deuterons dispersed in the Pd lattice. Their size can be estimated by examining the hot spots, cf. Fig. 4a. Using this approach Chubb [12] suggested 10^4–19^9 events occurring within a volume having a diameter of 100 Å.

The question, what is happening during the time separating complete saturation and onset of nuclear reaction, needed an answer. Fleischmann et al. [13] suggested that... *there are appropriate thermodynamic conditions for the formation of large clusters....* This statement can be extended to include self-organization which implies that there exists a volume element within the system having dimensions much larger than the characteristic molecular dimensions but smaller than the total volume of the system [14]. Within this volume fluctuations behave coherently thus modifying its microscopic behavior. At far from equilibrium, new structures, involving coherent behavior are formed and can be maintained only through a sufficient flow of energy [15]

Thermodynamic arguments imply that energy flow external to the clusters may affect their behavior. Indeed, as the solution temperature rises from 30 to 80°C, the hot spots are brighter and the mini-explosions stronger [11]. Since within this temperature range nuclear reaction rates are not affected, it means that either rate constant of the chain reaction increased or the cluster became larger. As a general proposition – a complex interplay of kinetic and thermodynamic quantities create conditions that allow the nuclear event to occur

5.2. The Letts–Hagelstein (L–H) protocol – a variant of co-deposition

The comparison of the co-deposition described in [1] and that presented in this communication can be best accomplished by the discussion of (i) process, (ii) product and (iii) performance.

(i) *Process*. Difference in (a) electrolyte composition, viz added H^+ ions, less $PdCl_2$, (b) in processing, e.g. co-deposition at 600 mA cm^{-2} results in very different kinetics of co-deposition. **(ii)** *Product*. The L–H protocol specifies the structure of the cathode, i.e. it requires the deposition of gold film prior to Pd + D co-deposition. **(iii)** *Performance*. Reproducible production of excess enthalpy.

If *to modify* means to introduce minor changes in either electrode preparation or cell operation, then based on information presented in [1] the L–H protocol is a new procedure rather then modification of another one. It does not matter how to call it. What matters is that cells using cathodes prepared by the L–H protocol can be operated at much higher current densities.

Acknowledgment

The experimental protocol developed in the SRAWAR laboratory yielded immediate and reproducible results in support of the Fleischmann–Pons claims. The results (excess enthalpy and tritium production) were presented to Dr Gordon who concluded that we have a new tool to investigate the nature of nuclear events occurring in the Pd/D–D_2O system. With his support, I and my Colleagues, were able to study, in addition to thermal behavior, electromagnetic radiation, transmutation and particle emission. This work could not have been done without the help and support of Dr Frank E Gordon, at that time a member of the US Navy Senior Executive Service.

References

[1] D. Letts and P. Hagelstein, *J. Condensed Matter Nuc. Sci.* **6** (2012) 44.
[2] S. Szpak, P.A. Mosier-Boss and J.J. Smith, *J. Electroanal. Chem.* **379** (1994) 121.
[3] S. Szpak, C.J. Gabriel, J.J. Smith and R.J. Nowak, *J. Electroanal. Chem.* **309** (1991) 273.
[4] S. Szpak, P.A. Mosier-Boss, S.R. Scharber and J.J. Smith, *J. Electroanal. Chem.* **380** (1995) 1.
[5] S. Szpak, P.A. Mosier-Boss, S.R.E. Scharber and J.J. Smith, *J. Electroanal. Chem*. **337** (1992) 147.
[6] H. Naohara, S. Ye and K. Uosaki, *J. Phys. Chem.* **B 102** (1998) 4366.
[7] T. Ohmori, K. Sohamaki, K. Hashimoto and A. Fujishima, *Chem. Lett.* 1991, p. 93, The Chemical Society of Japan.
[8] R. Defay and I. Prigogine, *Surface Tension and Absorption*, Longmans, London, 1966.
[9] J. Behm, *J. Chem. Phys.* **78** (1983) 7486.
[10] P.A. Mosier-Boss, *Il Nuovo Cimento* **112** (1999) 517.
[11] S. Szpak and F. Gordon, *J. Condensed Matter Nucl. Sci.* **12** (2013) 143.
[12] S.R.E. Chubb, Private communication, 1994.
[13] M. Fleischmann, S. Pons and F. Preparata, *Il Nuovo Cimento* **187A** (1994) 143.
[14] G. Nicolis, *Self-organization in Non-equilibrium Systems*, Wiley, Toronto, 1976.
[15] P. Glansdorff and I. Prigogine, *Thermodynamic Theory of Structure, Stability and Fluctuations*, Wiley Inter Science, London, 1971.